Paper:

Adaptive Gait for Large Rough Terrain of a Leg-Wheel Robot (Fourth Report: Step-Over Gait)

Shuro Nakajima and Eiji Nakano

The Department of Advanced Robotics, Chiba Institute of Technology
2-17-1 Tsudanuma, Narashino, Chiba 275-0016, Japan
E-mail: shuro.nakajima@it-chiba.ac.jp
[Received April 4, 2008; accepted April 4, 2008]

A leg-wheel robot has mechanically separated four legs and two wheels, and it performs high mobility and stability on rough terrains. The adaptive gait for large rough terrains of the leg-wheel robot is composed of three gait strategies. In this paper, the step-over gait, which is one part of the adaptive gait, is described. The proposed method is evaluated by simulations and experiments.
The point of the flow of the step-over gait is described. When the body reaches an obstacle, it does not come to advance easily. In this case, the robot can not always understand the height of the obstacle, since its forefeet sometimes do not touch it. Therefore, the robot raises its body as possible as it can, and gets over the obstacle. After getting over it, the body is lowered until it touches the ground. The system judges whether the body touches the ground by the information on load sharing ratio of legs.[1]

Keywords: mobile robot, adaptive gait, leg-wheel robot, rough terrain, motion control

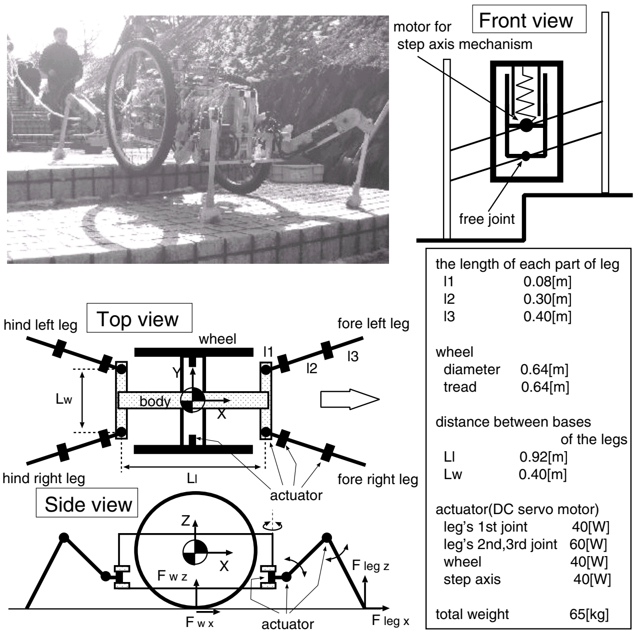

Fig. 1. A leg-wheel robot "Chariot 3".

1. Introduction

Legs, which enable robots to make arbitrary and irregular contacts with the ground, are capable of traversing a wide range of terrain including steps and slopes. Legs are mechanically complex, however, and positioning and leg control rely on recognition of the external environment, leaving a lot of tasks to solve for practical use.

We have been studying separated leg-wheel robots with 4 legs, two on the front side and two on the back side, each having 3 degrees of freedom (DOF), and with 2 independent wheels, one on each side, to enable robots to travel on unknown rough terrain but requiring less accuracy in recognition of the external environment and simpler control to make the robot practical [1, 2] (**Fig. 1**). We proposed basic movement control [1] for rough terrain with unevenness within ± 0.1 m (regular rough terrain) without using environment recognition sensors. Basic movement control does not cover all rough terrain since much terrain is more uneven than regular rough terrain.

We proposed 3 gait strategies for large rough terrain by classifying such terrain for leg-wheel robots to traverse [8]. We proposed step-up gait control [9] targeting rough terrain with ascending steps of 0.1-0.2 m. We proposed step-down gait control [10] targeting rough terrain with descending steps of 0.1-0.2 m. This study targets a step-over gait for protrusion of 0.1-0.2 m in rough terrain and describes control and movement ability for it.

The gait strategy Ohmichi et al. proposed for similar leg-wheel robots [3] was not targeted at unknown rough terrain. We target unknown rough terrain for leg-wheel robots in this study.

Conventional 4- and 6-leg-robots realized movement for rough terrain by force control using accurate force information from legs [4–7], but we propose movement control for unknown rough terrain using only internal sensors, i.e., angle sensors for every joint and positioning (pitch and roll) of the robot. We do not use external sensors because they are less accurate in natural environments such as slopes, steps, weedy or muddy land, and snow, with possible errors due to noise and other fac-

1. This paper is the full translation from the transactions of JSME Vol.72, No.721.

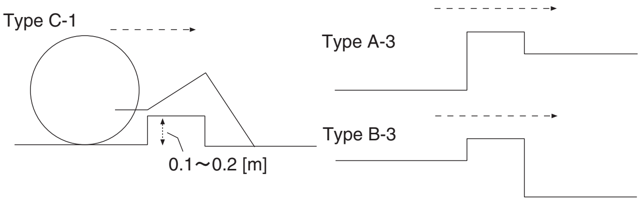

Fig. 2. Targeted rough terrain of the step-over gait.

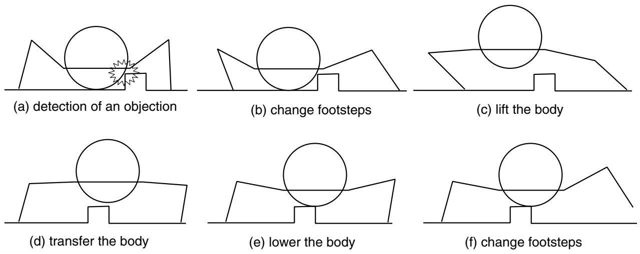

Fig. 3. Flow of the step-over gait.

tors. Our research policy holds that, for practical application, robots traversing unknown rough terrain should move based on information from internal sensors alone and that external sensors should be used to further enhance the capability.

2. Flow of Step-Over Gait

Figure 2 shows our targeted large rough terrain for step-over gait. Type C-1 represents a protruding surface of 0.1-0.2 m in height with a depth less than the distance between wheel contacts and leg contacts. Among those protruding surfaces, those with higher leg contacts to wheel contacts was defined as type A-3, and those with lower leg contacts as type B-3. Since classification and selection of the terrain were described previously [8], we do not detail them in this paper. As in the studies [8–10], steps are made up of planes.

A characteristic of the targeted terrain is that protrusion is situated between wheel contacts and leg contacts. With a protrusion between wheels and legs, legs may not land on the protrusion, indicating that height information obtained through leg contacts is not necessarily available to assess the height of the protrusion. So, we determined that the step-over gait was to be conducted with the maximum height for the robot to take. Specifically, when detecting a protrusion, the robot stops (**Fig. 3(a)**) and repositions the legs (preparatory leg repositioning: **Fig. 3(b)**). Then, the robot lifts its body to the maximum height (**Fig. 3(c)**). After lifting, the robot advances the body by one stride (**Fig. 3(d)**), lowers the body until it contacts the ground (**Fig. 3(e)**), repositions the legs (**Fig. 3(f)**) and then returns to the normal gait.

The above step-over gait needs to lift the body to the maximum height regardless of the height of the protrusion. This takes more time and energy than those would be necessary. It is understood that, if a protrusion is not

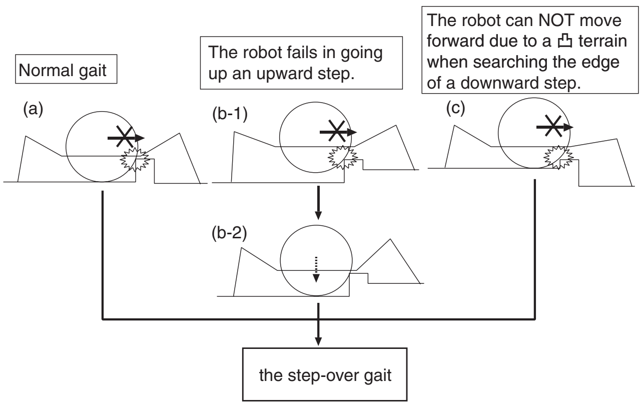

Fig. 4. Three cases in which the robot uses the step-over gait

overstridden by the step-over gait, the protrusion is physically difficult to stepped over with the dimensions of the robot. Step-over gaits for type A-3 and type B-3 terrain, as detailed later, are intended as complemental gaits for step-up gait [9] and step-down gait [10] if they are unable to cope with obstacles.

The step-over gait can be understood that the gait is useful for the terrain for which height information is difficult to obtain as in the case of a protrusion or for the terrain that cannot be traversed by either step-up or step-down gait because the step-over gait requires more time and energy even though it provides high traverse capability.

3. Step-Over Gait Control

3.1. Switching to Step-Over Gait

When we consider traverse over targeted terrain (**Fig. 2**), there are 3 cases in which the robot switches the gait to the step-over gait (**Fig. 4**). In **Fig. 4(a)**, the robot encounters an obstacle and is unable to go forward with low estimated step height H_e [9]. The robot is to determine that it is unable to go forward, in the same manner as in the case of the step-up gait [9] in detecting an ascending step start position, when the smallest of the two wheels in deviation between rotation angle θ_{wi} and targeted angle θ_{wdi} of wheel i exceeds threshold $\Delta_{w\min}$ (Eq. (1)).

$$\min(\delta_{wi}) > \Delta_{w\min} \quad (i = 1, 2) \quad . \; . \; . \; . \; . \; . \; . \; (1)$$

The reason for using the smallest deviation was detailed in the previous paper [9] and is not be detailed in this paper. In short, using the smallest wheel deviation matched actual cases (in which a robot was unable to go forward) very well. We determined that an obstacle be detected when more than 80% of time series data were out of threshold during a period of 0.45 s to avoid erroneous detection instead of using single data from a processing cycle, which may increase detection error. The values were determined experimentally.

The robot is unable to determine at this time which, an ascending step or protrusion, interferes. The robot will

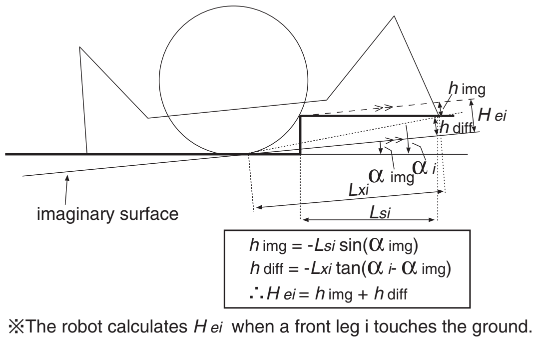

Fig. 5. Estimation of a step height.

obtain estimated step height H_{ei} during a preparatory leg repositioning after detection by Eq. (1), and select either step-up gait [9] or step-over gait using H_{ei}. Specifically, if each of H_{ei} is smaller than threshold $\Delta_{\text{step over}}$ ($= 0.05$: experimentally determined) at the beginning of the all-leg-support gait, the step-over is selected and the step-up gait is selected for the rest (Eq. (2)).

$$\max(H_{ei}) < \Delta_{\text{step over}} \quad (i = 1, 2) \quad \ldots\ldots \quad (2)$$

Estimated step height H_{ei} for front leg i means a vertical height from the imaginary surface [1] (**Fig. 5**), which is determined based on robot body angle and leg positions (for details, refer to the paper [9]).

With the case in **Fig. 4(b-1)**, a protrusion higher than the estimated step height may interfere with the robot during ascent of the protrusion by the step-up gait so it can not raise the body as targeted. To address this problem, the robot switches the gait to the step-over gait when the sum of angular deviations δ_{wi} for both wheels exceeds threshold $\Delta_{w\text{up}}$. The reason for using the sum of the deviations, we thought it better experimentally to use the sum rather than using deviations form one wheel, since the deviation of each wheel may vary by surface condition. We experimentally determined $\Delta_{w\text{up}} = 30°$. When the sum of wheel angular deviations δ_{wi} exceeds threshold $\Delta_{w\text{up}}$ during step-up gait, the robot lowers the body it has raised (**Fig. 4(b-2)**), and then repositions the legs (**Fig. 3(b)**) to switch to the step-over gait.

With the case in **Fig. 4(c)**, the robot becomes unable to go forward during a search for the edge of a descending step in step-down gait [10]. This case also switches the gait to the step-over gait when the sum of angular deviations δ_{wi} for both wheels exceeds threshold $\Delta_{w\text{down}}$. We experimentally determined $\Delta_{w\text{down}} = 25°$.

3.2. Wheel Control

This section describes wheel control for the step-over gait. The wheels are stopped when the robot body is lifted or lowered (**Fig. 3(c)**, **(e)**). When the robot advances the body (**Fig. 3(d)**), the wheels may contact the ground depending on the height of the ground, so, the wheels are rotated corresponding to the targeted velocity.

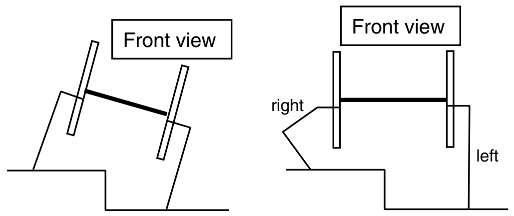

(a) Each leg tip position is set to the lowest limit.
(b) Right leg is set to upper position than the lowest limit.

Fig. 6. Motion for the step-over gait in the case of a surface with different level on either side.

3.3. Leg Control

When the body is lifted (**Fig. 3(c)**), the legs are lowered to the lowest limit so that the body is raised to the maximum height. However, when the heights of right and left leg contacts differ as in **Fig. 6(a)**, if all legs were lowered to the lowest, the robot might tumble. So, the legs are lowered in such manner as indicated in **Fig. 6(b)**. This is achieved by lowering the legs until a leg reaches to the lowest limit while maintaining the height difference between right and left leg contacts at the beginning of the body lifting. Front and rear legs are controlled independently.

When advancing the body (**Fig. 3(d)**), the leg positions in the direction of the z-axis in the body coordinates are fixed. The leg control in the direction of the x and y directions in the body coordinates is performed by the event-driven gait algorithm [2] based on given velocity by the operator.

When the body is lowered (**Fig. 3(e)**), the legs are lifted simultaneously until wheels contact the ground.

The leg compliance in the direction of the z-axis is described below. Determination whether wheels contact the ground is made in **Fig. 3(e)** by monitoring leg load sharing ratio k_{leg} [9], as was used in the step-down gait in the measure for under estimated step height [10]. Specifically, a wheel is determined to have contacted the ground when k_{leg} becomes smaller than threshold $R_k = 0.5$ (experimentally determined). Leg load sharing ratio k_{leg} represents the ratio of the weight supported by all legs to the entire weight of the robot. When the body is lowered, if the stiffness is set too high, the transition time from leg support to wheel support will be short, making it difficult to detect the time at which the body lowering should be terminated. So, the leg compliance was set so that deviations of actual positions from the targets would be equal to basic value Δ_s used in the normal gait [1]. In other words, the leg compliance K_{zd} indicated by the following equation is set so that the body weight W is supported by the four legs and deviations of leg positions from the targets in the direction of the z-axis would be equal to basic value Δ_s.

$$K_{\text{zd}} = W / n\Delta_s \quad \ldots\ldots\ldots\ldots \quad (3)$$

where $n (= 4)$ represents the number of the support legs. As the compliance setting immediately after preparatory leg repositioning differs from the value indicated by Eq. (3), the compliance of each leg is changed at a same

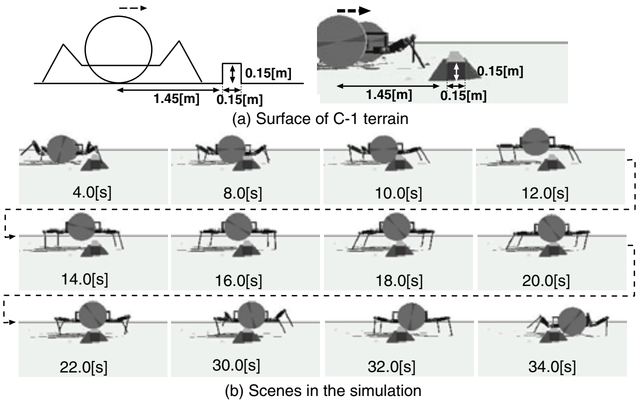

Fig. 7. Scenes in the simulation when moving on Type C-1 terrain.

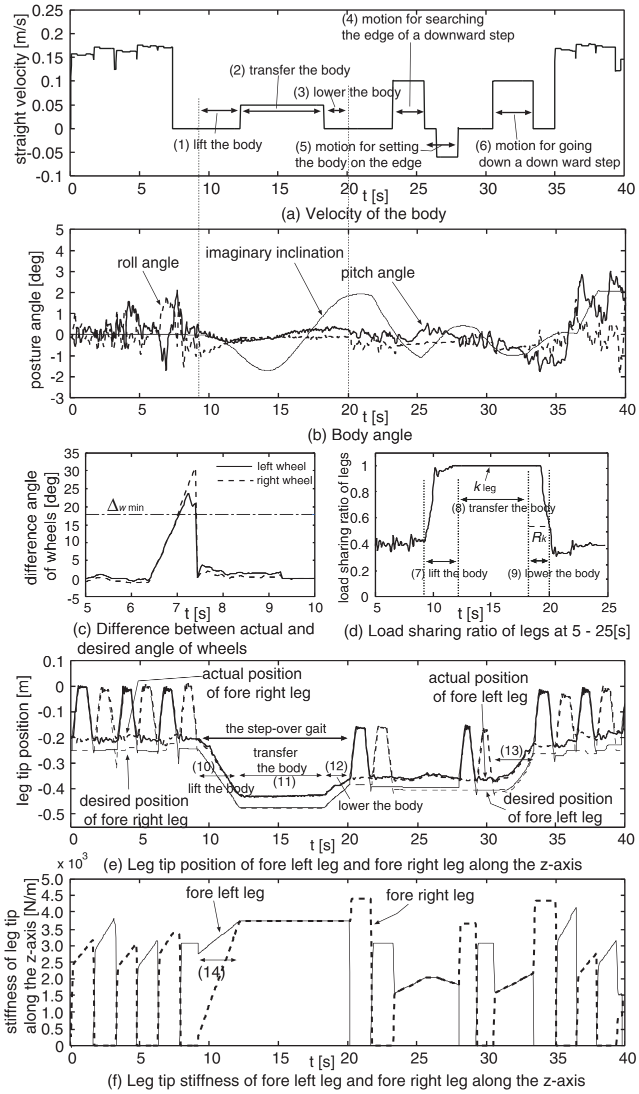

Fig. 8. Simulation data (Type C-1).

rate in the period of **Fig. 3(c)** so that it becomes equal to that of Eq. (3) when in the position of **Fig. 3(d)**.

4. Simulation

We verify in this section that the proposed gait enables robots to traverse the targeted large rough terrain. Simulation and experiment conditions were as follows: swing leg speed was 0.5 m/s, swing leg lifting height 0.2 m, maximum leg lowering for a swing leg to land 0.4 m, stride width 0.3 m, basic deviation of actual leg positions from targets $\Delta_s = 0.043$ m, stiffness for all legs and for suspension in the direction of the z-axis 7500 N/m, the basic load sharing ratio between legs and wheels 1:1, P and D gains for wheel rotation control 80 Nm/rad and 20 Nm/rad/s, and P and D gains for step axis control 1000 Nm/rad and 100 Nm/rad/s. The gait was a trot [2] and the environment was assumed to be unknown. We used the Open Dynamics Engine (ODE) to dynamically simulate assuming rigid contact between the legs and ground and the wheel and ground. The friction coefficient between the legs and ground was set at 0.4 and that between the wheels and ground at 0.7.

4.1. Type C-1 Terrain

Simulation was conducted with an unknown protrusion of 0.15 m in height and 0.15 m in width (**Fig. 7(a)**) and simulation results are shown in **Fig. 7(b)**. The robot ascended the protrusion with the step-over gait and then descended with step-down gait [10].

Figures 8(a)-**(f)** show the data. **Fig. 8(a)** shows the target translational velocities. The robot raised its body to the maximum height (period (1)), advanced by one stride with the body raised (period (2)), and lowered the body to land on the protrusion (period (3)). Then, the robots descended the protrusion with the step-down gait (periods (4)-(6)).

Figure 8(b) shows transition of the body pitch and roll angles and the inclination of the imaginary surfaces. Since all legs were lowered in the step-over gait as in **Fig. 6**, body angles were roughly constant during the step-over gait, and for the rest of the period, body pitch angles followed the inclination of the imaginary surface and body roll angles were kept horizontal.

Figure 8(c) shows wheel angular deviations. When the wheels contacts the protrusion at time 6 s, the deviations for both wheels started increasing.

Figure 8(d) shows the transition of leg load sharing ratio k_{leg}. It increased when the body was lifted (period (7)) and was roughly equal to 1 during body advancement (period (8)). k_{leg} then decreased when the body was lowered and landed on the protrusion. When k_{leg} becomes lower than threshold R_k, the robot goes into terminating leg reposition.

Figure 8(e) shows the target and actual front (right and left) leg positions in the direction of the z-axis in body coordinates. Period (10) corresponds to body lifting, period (11) to body advancement, and period (12) to body lowering. Target values for both legs were lowered to the lower limit (-0.475 m). The period (13) corresponds to all-leg-support period in the step-down gait.

Figure 8(f) shows stiffness of the fore right and fore left legs in the direction of the z-axis in the body coordinates.

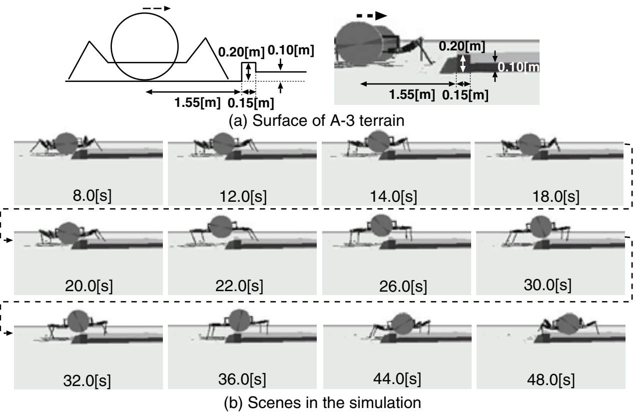

Fig. 9. Scenes in the simulation when moving on Type A-3 terrain.

The stiffness was changed properly based on the deviations between the actual and target leg positions. Stiffness in period (14) was for body lifting and it changes from the stiffness for the normal gait to that for the step-over gait continuously.

4.2. Type A-3 Terrain

Simulation was conducted with an unknown protrusion of 0.20 m in height and 0.15 m in width located at the beginning of a 0.10 m step (**Fig. 9(a)**) and simulation results are shown in **Fig. 9(b)**. The robot started with the step-up gait with recognition of a 0.10 m ascending step (the estimated step height [9] $H_e = 0.089$ for the step-up gait), but switched to the step-over gait when detected that it was unable to ascend the step. Then, it ascended the protrusion with the step-over gait and descended the protrusion with the step-down gait.

Figures 10(a)-(f) show the data. **Fig. 10(a)** shows target translational velocities. The period (1) corresponds to the duration of the step-up gait. Because the estimated step height is lower than the actual height, the sum of wheel angular deviations δ_{wi} exceeded threshold $\Delta_{w\mathrm{up}}$ (period (6) in **Fig. 10(c)**) and the robot switched the gait to the step-over gait. The period (2) in **Fig. 10(a)** corresponds to a preparatory period for step-over gait in which the once-lifted body was lowered. Period (3) corresponds to a preparatory leg repositioning for the step-over gait and period (4) to the step-over gait. The robot descended from the protrusion with the step-down gait (Period (5)).

Figure 10(b) shows the body pitch and roll angles and the inclination of the imaginary surfaces. As in type C-1 terrain, the body angles were roughly constant during the step-over gait (period (4) in **Fig. 10(a)**) and for the rest of the period, body pitch angles followed the inclination of the imaginary surface and body roll angles were kept horizontal.

Figure 10(c) shows angular deviations for both wheels during the step-up gait in all-leg-support gait [9]. Upon determination to switch to the step-over gait (period (6)), the angular deviations once became zero since the target wheel angles were reset to the actual angles.

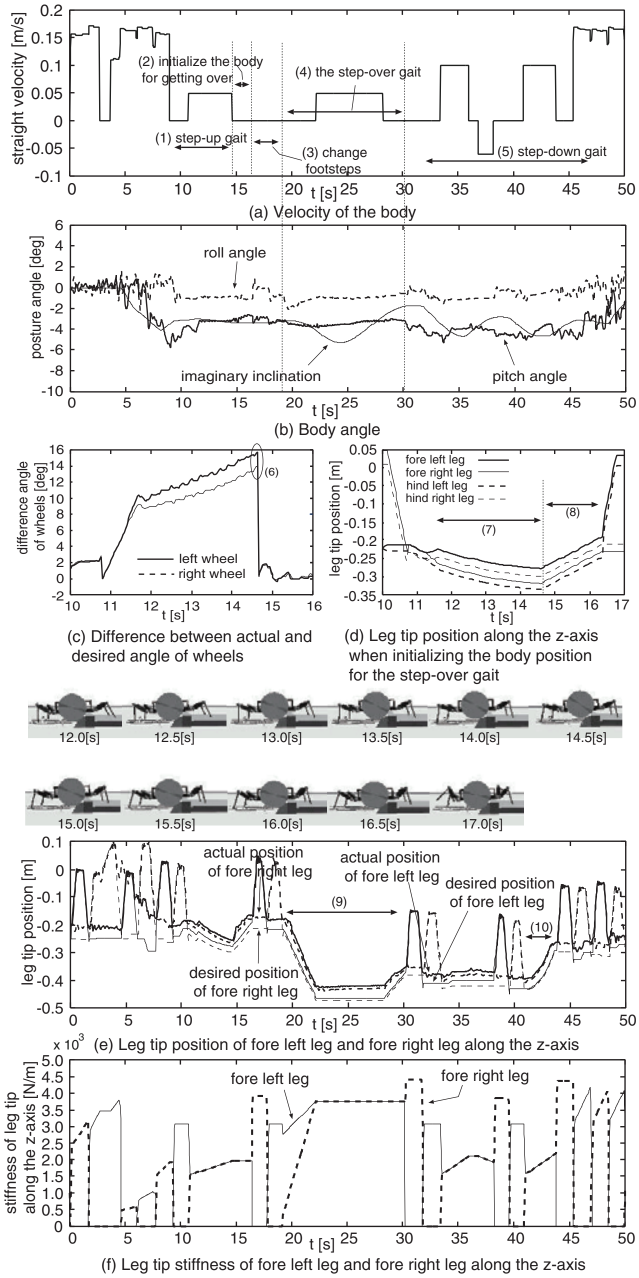

Fig. 10. Simulation data (Type A-3 terrain).

Figure 10(d) shows target leg positions in the direction of the z-axis in the body coordinates during the transition period from the step-up gait to the step-over gait. The body was lifted in the step-up gait in period (7) in **Fig. 10(d)**, but after period (6) in **Fig. 10(c)** the leg positions were lifted to lower the body to prepare the step-over gait (period (8) in **Fig. 10(d)**). Pictures under **Fig. 10(d)** show motions in this period. The body is lowered for the same distance as lifted in the step-up gait.

Figure 10(e) shows the target and actual front (right and left) leg positions in the direction of the z-axis in body coordinates. Period (9) corresponds to step-over movement in the step-over gait and period (10) corresponds to all-leg support gait in the step-down gait.

Figure 10(f) shows stiffness of the right and left legs in the direction of the z-axis in the body coordinates.

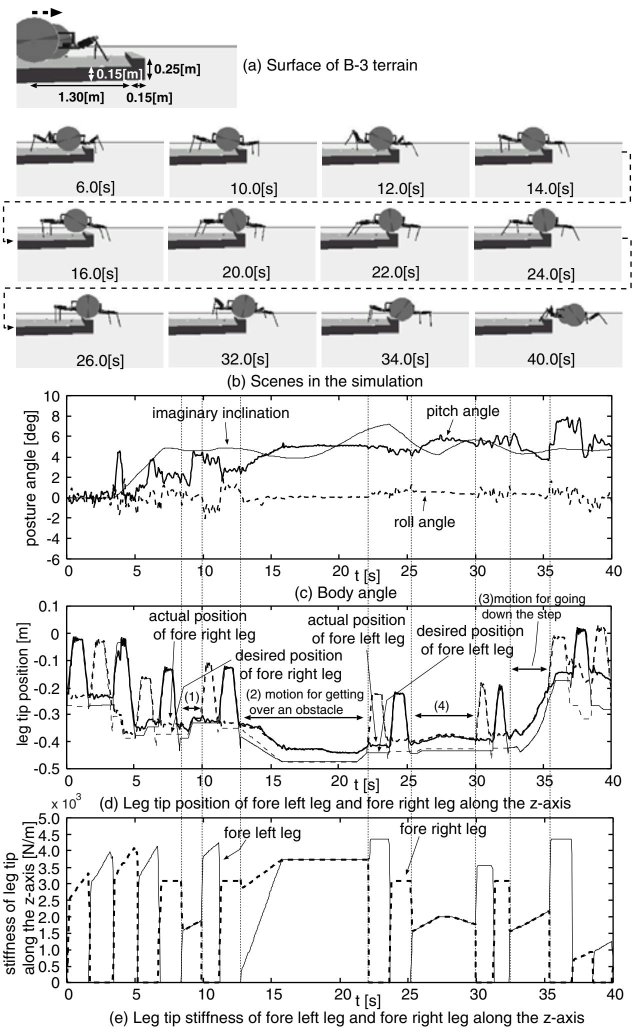

Fig. 11. Simulation data when moving on Type B-3 terrain.

4.3. Type B-3 Terrain

Simulation was conducted with a protrusion of 0.10 m in height and 0.15 m in width located at the beginning of a 0.15 m descending step (**Fig. 11(a)**) and simulation results are shown in **Fig. 11(b)**. The robot started a search for the edge of a descending step [10] before the step. During the search (period (1) in **Fig. 11(d)**), the robot encountered the protrusion. As the wheel angular deviations increased, it detected the protrusion and switched into the step-over gait. It ascended the protrusion with the step-over gait (period (2) in **Fig. 11(d)**) and descended with the step-down gait (period (3) in **Fig. 11(d)**).

Figure 11(c) shows transition of the body pitch and roll angles and the inclination of the imaginary surfaces. **Fig. 11(d)** shows the target and actual front (right and left) leg positions in the direction of the z-axis in body coordinates. The deviations between the target and actual positions are attributable to compliance set to the legs. **Fig. 11(e)** shows stiffness of the right and left legs in the direction of the z-axis in the body coordinates. Period (4) in **Fig. 11(d)** corresponds to the searching motion for the edge of a descending step in the step-down gait to descend the body from the protrusion.

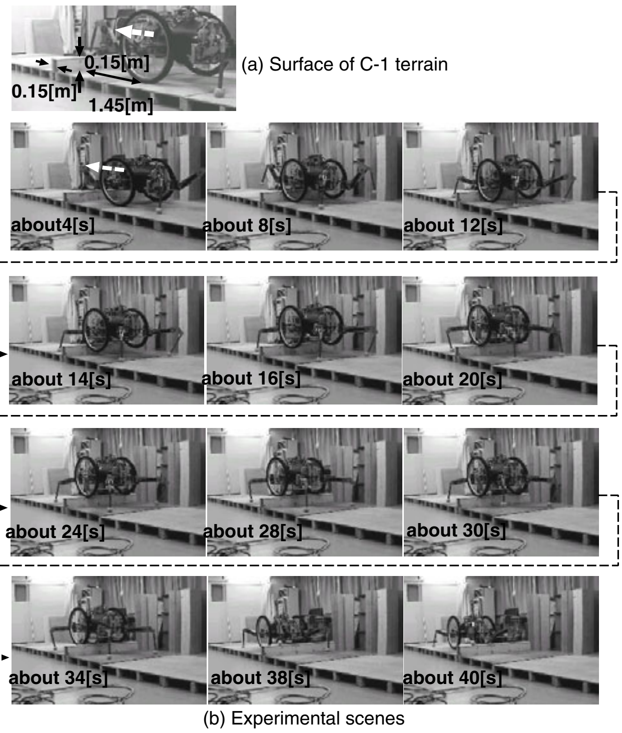

Fig. 12. Experimental scenes when moving on Type C-1 terrain.

These results demonstrate that combination of step-down and step-over gaits enabled the robot to traverse type B-3 terrain.

5. Traverse Experiment on Rough Terrain

Experiments were conducted with the targeted terrain (**Fig. 2**) and terrain with different lateral step heights. We conducted simulation and experiments with detailed data acquisition, however, due to space limitation, we show a part of them. Although diagonal entrance to an obstacle and traverse over slanted steps were described in the previous papers [9, 10], we curtailed these discussion on the effects over these surfaces because they can be adequately deduced from the study in the papers.

5.1. Type C-1 Terrain

Experiments were conducted with terrain in **Fig. 12(a)**. Topography was the same as in **Fig. 7**. **Fig. 12(b)** shows photos in the experiments with the actual robot (robot moving from the lower right to the upper left), demonstrating successful ascent of the protrusion with the step-over gait (around time 14 to 20 s in **Fig. 12(b)**) and descent with the step-down gait (around time 34 to 38 s in **Fig. 12(b)**)

5.2. Type A-3 Terrain

Experiments were conducted with terrain in **Fig. 13(a)**. Topography was the same as in **Fig. 9**. **Fig. 13(b)** shows photos in the experiments (robot moving from the lower

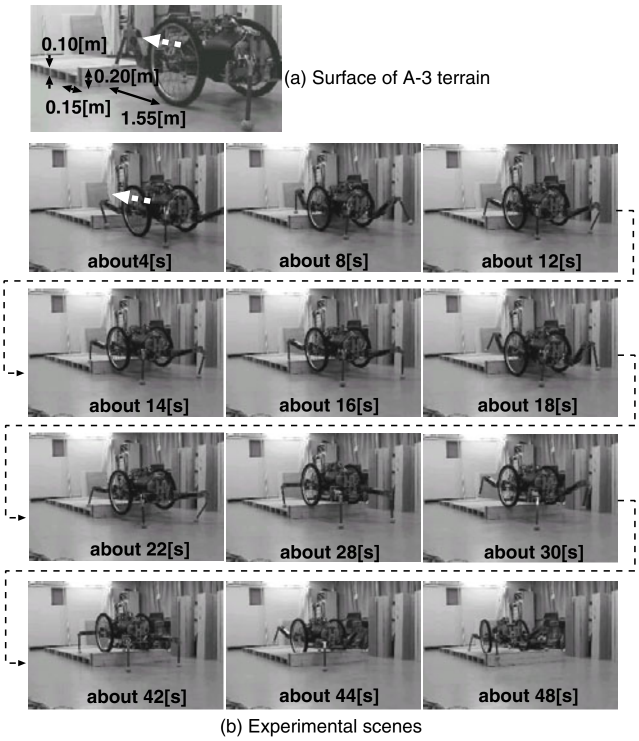

Fig. 13. Experimental scenes when moving on Type A-3 terrain.

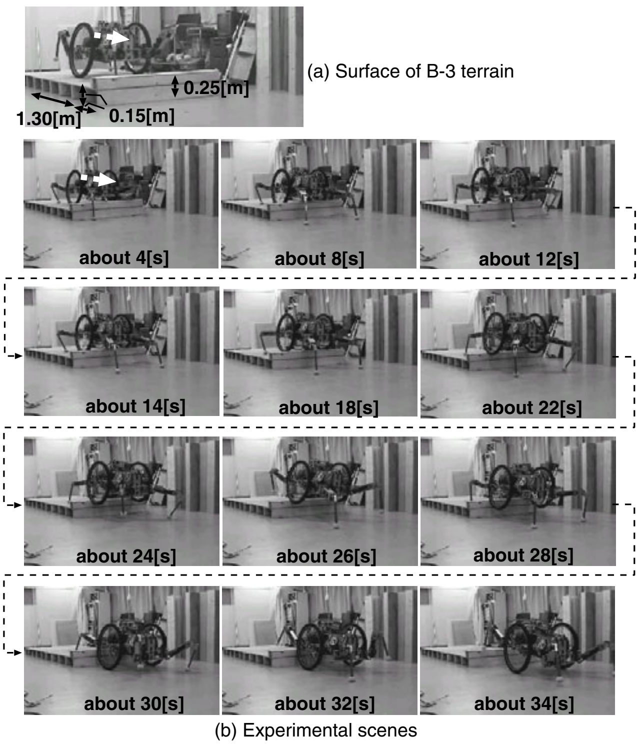

Fig. 14. Experimental scenes when moving on Type B-3 terrain.

right to the upper left), demonstrating successful switching to the step-over gait upon determination that it was unable to ascend the protrusion with the step-up gait (around time 14 s in **Fig. 13(b)**). The robot ascended the protrusion (around time 22 to 28 s in **Fig. 13(b)**) and descended with the step-down gait (around time 42 to 44 s in **Fig. 13(b)**).

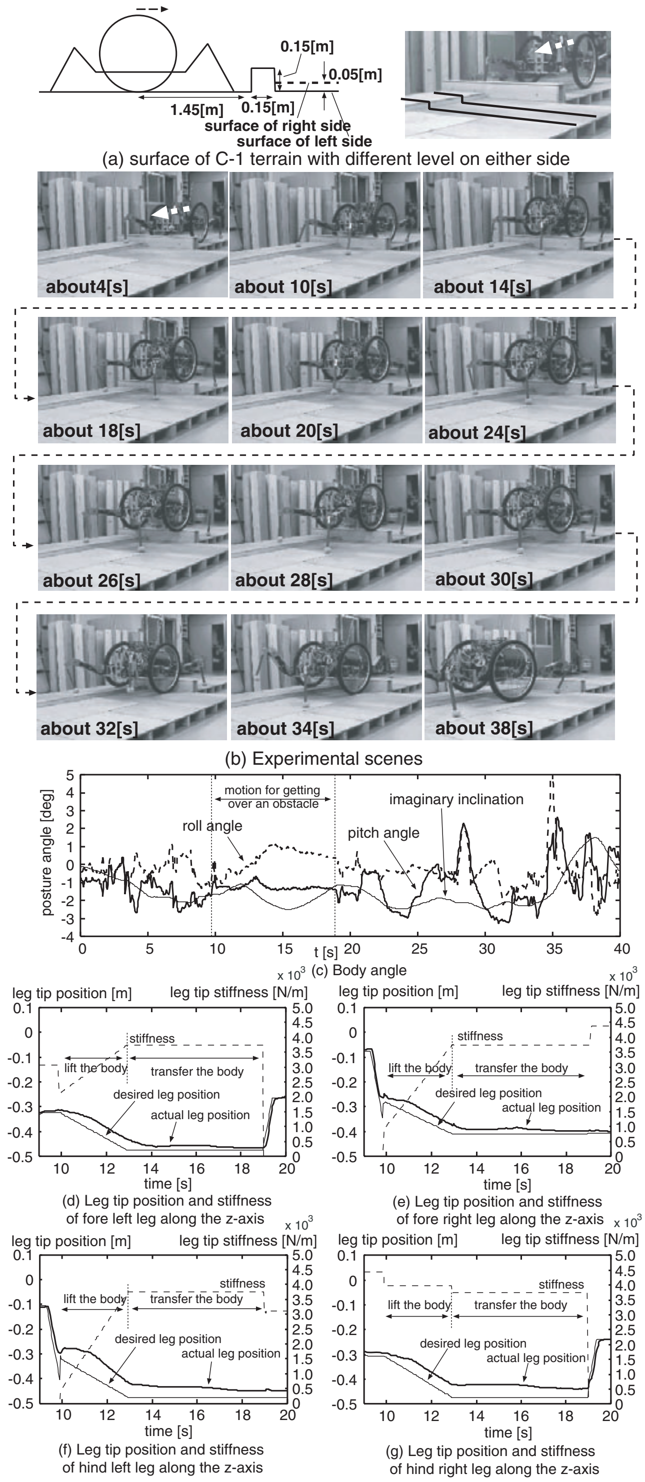

Fig. 15. Experimental scenes when moving on a terrain with different level on either side.

5.3. Type B-3 Terrain

Experiments were conducted with terrain in **Fig. 14(a)**. Topography was the same as in **Fig. 11**. **Fig. 14(b)** shows photos in the experiments (robot moving from the upper left to the lower right), demonstrating switching to the step-over gait upon determination that it was unable to go forward during the search for the edge of a descending step (around time 8 s in **Fig. 14(b)**) in the step-down gait. The robot then ascended the protrusion (around time 14 to 22 s in **Fig. 14(b)**) and descended with the step-down gait (around time 26 to 30 s in **Fig. 14(b)**).

5.4. Terrain with Laterally Different Step Heights

Experiments were conducted with terrain with laterally different step heights (**Fig. 15(a)**). The right surface was 0.05 m higher than that of the left. **Fig. 15(b)** shows photos in the experiments (robot moving from the upper right to the lower left). It demonstrated that the robot achieved stable body lifting in the step-over gait even with different lateral step heights.

Figure 15(c) shows transition of the body pitch and roll angles and the inclination of the imaginary surfaces. The results demonstrate that the robot achieved stable traverse over the terrain with laterally different step heights without showing significant tilts in the rolling direction. The large peak around time 35 s is attributable to shocks from rear legs landing on the protrusion.

Figures 15(d)-(g) show the target and actual front (right and left) leg positions in the direction of the z-axis in body coordinates and stiffness of the legs during the step-over gait. They indicate that the target positions for the right and left legs differ by the difference between right and left step heights. As for the rear legs, they show about the same position since there is no difference in height of the surface.

6. Conclusions

We have proposed control for step-over gait for leg-wheel robots as an adaptive gait for large rough terrain. Traversing was demonstrated by both simulation and experiments on large rough terrain using the proposed step-over gait. Simulation and experiments for all targeted terrain confirmed that the proposed gait enabled the robot to successfully traverse terrain (part of results reported due to space limitation).

We will verify that leg-wheel robots can traverse general rough terrain including various types of rough terrain successively by systematic cooperation between normal gait and the proposed three gait strategies (reported in this and previous papers). We will report the outcome in other papers.

References:

[1] S. Nakajima et al., "The Motion Control Method for a Leg-wheel Robot on Unexplored Rough Terrains," Journal of the Robotics Society of Japan, Vol.22, No.8, pp. 1082-1092, 2004.

[2] S. Nakajima et al., "Trot and Pace Gaits based on the Predictive Event Driven Method for a Leg-wheel Robot," Journal of the Robotics Society of Japan, Vol.22, No.8, pp. 1070-1081, 2004.

[3] T. Ohmichi and T. Ibe, "Development of Vehicle with Legs and Wheels," Journal of the Robotics Society of Japan, Vol.2, No.3, pp. 244-251, 1984.

[4] S. M. Song and K. J. Waldron, "Machines That Walk: The Adaptive Suspension Vehicle," MIT Press, 1989.

[5] D. M. Gorinevsky and A. Shneider, "Force Control of Legged Vehicles over Rigid and Soft Surfaces," Int. Journal of Robotics Research, Vol.9, No.2, pp. 4-23, 1990.

[6] J. E. Bares and W. L. Whittaker, "Configuration of Autonomous Walkers for Extreme Terrain," The Int. Journal of Robotics Research, Vol.12, No.6, pp. 535-559, 1993.

[7] T. Hori et al., "Force Control for Hexapod Walking Robot with Torque Observer," Proc. of the Int. Conf. on Intelligent Robots and Systems, pp. 1294-1300, 1994.

[8] S. Nakajima and E. Nakano, "Adaptive Gait for Large Rough Terrain of a Leg-Wheel Robot (First Report: Gait Strategy)," Journal of Robotics and Mechatronics, Vol.20, No.5, pp. 801-805, 2008.

[9] S. Nakajima and E. Nakano, "Adaptive Gait for Large Rough Terrain of a Leg-Wheel Robot (Second Report: Step-Up Gait)," Journal of Robotics and Mechatronics, Vol.20, No.6, pp. 913-920, 2008.

[10] S. Nakajima and E. Nakano, "Adaptive Gait for Large Rough Terrain of a Leg-Wheel Robot (Third Report: Step-Down Gait)," Journal of Robotics and Mechatronics, Vol.21, No.1, pp. 12-20, 2009.

Name:
Shuro Nakajima

Affiliation:
Ph.D. (Information Science), Associate Professor, The Department of Advanced Robotics, Chiba Institute of Technology

Qualification:
Professional Engineer (Mechanical Engineering)

Address:
2-17-1 Tsudanuma, Narashino, Chiba 275-0016, Japan

Brief Biographical History:
1997- East Japan Railway Company
2005- Future Robotics Technology Center, Chiba Institute of Technology
2006- The Department of Advanced Robotics, Chiba Institute of Technology

Main Works:
• S. Nakajima and E. Nakano, "Adaptive Gait for a Leg-Wheel Robot Traversing Rough Terrain (Second Report: Step-Up Gait)," Journal of Robotics and Mechatronics, Vol.20, No.6, pp. 913-920, 2008.

Membership in Academic Societies:
• Institute of Electrical and Electronics Engineers (IEEE)
• The Japan Society of Mechanical Engineers (JSME)
• The Robotics Society of Japan (RSJ)
• Japan Society of Kansei Engineering (JSKE)
• The Institute of Professional Engineers, Japan (IPEJ)

Name:
Eiji Nakano

Affiliation:
Doctor of Engineering, Professor, The Department of Advanced Robotics, Chiba Institute of Technology

Address:
2-17-1 Narashino, Chiba 275-0016, Japan

Brief Biographical History:
1970 Graduated, Postgraduate Course of University of Tokyo
1970- Senior Researcher, Mechanical Engineering Laboratory
1987- Professor, Tohoku University
2005- Professor, Chiba Institute of Technology

Main Works:
• E. Nakano et al., "Leg-Wheel Robot: A Futuristic Mobile Platform for Forestry Industry," 1993 IEEE/Tsukuba Industrial Workshop on Advanced Robotics, 1993.

Membership in Academic Societies:
• Robotics Society of Japan (RSJ)
• Japan Society of Mechanical Engineers (JSME)
• Society of Instrument and Control Engineers (SICE)
• Society of Biomechanism (SOBIM)